



Changes of microbial cell survival, metabolic activity, efflux capacity, and quorum sensing ability of *Aggregatibacter actinomycetemcomitans* due to antimicrobial photodynamic therapy-induced bystander effects

Marzie Mahdizade-ari^a, Maryam Pourhajibagher^{b,*}, Abbas Bahador^{a,*}

^a Department of Microbiology, School of Medicine, Tehran University of Medical Sciences, Tehran, Iran

^b Dental Research Center, Dentistry Research Institute, Tehran University of Medical Sciences, Tehran, Iran

ARTICLE INFO

Keywords:

Aggregatibacter actinomycetemcomitans
Curcumin
Bystander
Periodontitis
Peri-implantitis
Antimicrobial photodynamic therapy

ABSTRACT

Background: The bystander effects, whereby naive (bystander) microbial cells near microbial cells directly exposed to certain treatment show responses that would not have happened in the absence of the directly targeted microbial cells, is recently documented in the field of microbiology. In this article, we discuss that substantial bystander responses are also observed after antimicrobial photodynamic therapy (aPDT) using curcumin (Cur). **Materials and methods:** Bystander effects induced by whole bacterial cell suspension (WBCS^T), cell-free supernatants fluid (CFSF^T), and bacterial cell pellet (BCP^T) obtained from *A. actinomycetemcomitans* culture treated with Cur-aPDT on cell survival, quorum sensing (QS) ability, metabolic activity and efflux capacity of *A. actinomycetemcomitans* were determined using microbial viability assay, *Escherichia coli*-based bioassay, XTT reduction method, and ethidium bromide (EtBr) accumulation assay, respectively.

Results: *A. actinomycetemcomitans* cell survival reduced by 82.7% (P = 0.001) and 76.2% (P = 0.01) after exposure to WBCS^T and CFSF^T, respectively. The *A. actinomycetemcomitans* population increased by 5.5% (P = 0.7) after exposure to BCP^T. Bacterial metabolic activity decreased by 42.6% (P = 0.02), 35.3% (P = 0.03), and 9.4% (P = 0.5) after exposure to WBCS^T, CFSF^T, and BCP^T, respectively. *A. actinomycetemcomitans* exposed to WBCS^T, CFSF^T, and BCP^T showed a reduction of 83.2% (P = 0.001), 77.2% (P = 0.01) and 21.9% (P = 0.09) in the QS mediator compared to the WBCS^U, CFSF^U, and BCP^U of untreated *A. actinomycetemcomitans*, respectively. No significant change of the EtBr accumulation was observed in the three preparations of the Cur-aPDT-treated culture (i.e. WBCS^T, CFSF^T, and BCP^T) compared to their respective controls.

Conclusions: The results of the current study revealed that Cur-aPDT could significantly reduce microbial cell survival, cell metabolic activity, efflux capacity, and QS ability through the bystander effects. As a result, the bystander effects of Cur-aPDT along with the direct effect of Cur-aPDT can enhance the efficiency of aPDT as an adjunct therapeutic strategy for treatment of local infections.

1. Introduction

Colonization of perio-pathogenic microorganisms in the gingival sulcus, formation of microbial plaque, and reduced number of periodontal health-related bacteria are the main local factors in developing periodontitis and peri-implantitis [1–3]. Among all perio-pathogenic bacteria, *Aggregatibacter actinomycetemcomitans* is extremely important for having several virulence factors with a wide range of activities, which enable it to persistently colonize the oral cavity, evade host defenses, invade periodontal tissues, initiate connective tissue destruction,

and interfere with tissue healing [4].

Anti-infective therapy is one of the key steps in managing periodontitis and peri-implantitis in non-surgical (initial) therapy intending to reduce periodontal pathogens [3]. Given the fact that systemic administration and local delivery of antibiotics are associated with an increased level of antimicrobial resistance in sub-gingival microbiome [5], the photodynamic deactivation method or antimicrobial photodynamic therapy (aPDT), a light-based approach, has been introduced to cure local infections, such as periodontitis and peri-implantitis, as a complementary therapy in recent years [6]. In this method, a light

* Corresponding author at: Department of Microbiology, School of Medicine, Tehran University of Medical Sciences, Keshavarz Blvd, 100 Poursina Ave., Tehran, Iran.

** Corresponding author.

E-mail addresses: pourhajibagher@alumnus.tums.ac.ir (M. Pourhajibagher), abahador@sina.tums.ac.ir (A. Bahador).

<https://doi.org/10.1016/j.pdpdt.2019.04.021>

Received 8 October 2018; Received in revised form 22 April 2019; Accepted 22 April 2019

Available online 24 April 2019

1572-1000/ © 2019 Elsevier B.V. All rights reserved.

sensitive material, also known as a photosensitizer, produces reactive oxygen species (ROS) after activation with the corresponding light, which are able to kill microorganisms and modulate microbial virulence factors [7,8].

It has been shown that the use of photosensitizers, such as curcumin (Cur), in aPDT can significantly reduce the number of bacteria, including *A. actinomycetemcomitans* [9]. However, due to the received aPDT, pathogenic microorganisms may not completely be eradicated and may produce and/ or release compounds after receiving aPDT, which not only may not inactivate or eradicate the microorganisms growing in the community context of their surrounding microenvironment, but also may affect a broad range of their virulence factors, pathogenicity, and resistance to antimicrobial agents in a process called the "bystander effects" [10,11].

Most definitions of the bystander effects in the literature are presented by the authors themselves, typically framed in the context of the data revealed in that study [12]. Tedijanto et al. recently studied the "bystander effects" in the field of microbiology in a study entitled "bystander selection for antibiotic resistance" [13]. Accordingly, untreated susceptible (bystander) bacterial cells (microbiome) that are not directly targeted by the antibiotic exhibit antimicrobial resistance via horizontal gene acquisition when they are in close proximity to the treated pathogenic bacteria causing an infection (target pathogens). Tedijanto et al. [13] showed that in "bystander selection", the bystander microbial cells exhibited an antibiotics-resistant phenotype upon receiving resistant encoding genes known as "signals" from the targeted resistant microorganisms. Warburton et al. [14] also reported that the bystander cells were involved in potentiation of resistance to doxycycline through acquisition of conjugative transposon from doxycycline-resistant *Streptococcus oralis* containing CTn 6002 to untreated doxycycline-susceptible *Streptococci* spp. (*S. sanguinis* and *S. cristatus*) during systemic antimicrobial treatment of periodontitis in humans.

The bystander cells in oral microbiome exhibit many types of complex interactions via intercellular interactions, either from co-resident bacterial species or from exogenous sources. The intercellular interactions contribute to the fitness of the bacterial host within the human oral cavity [15,16].

Subsequent studies identified several mechanisms for intercellular communication, such as direct contact of treated cells with untreated cells and medium mediated signaling including the release of soluble factors from treated cells that diffuse through the medium and affect untreated cells [17].

Although the accepted paradigm of aPDT-induced diverse cellular changes in microorganisms results from its direct effect on the targeted microbial cells [18], aPDT can indirectly affect the non-directly targeted (bystander) microbial cells via intercellular signaling that abandoned from the targeted microorganisms [10]. Bystander selection can covert some nearby untreated microbial cells to epigenetically activated ones. The microbial cells in the new state are more prone to behaviors than normal cells and therefore show increased or reduced responses for many end points, including cell survival and expression of virulence factors. In situations where bystander signals predominantly reduce virulence factors, removing the pathogenicity of many potentially virulent bacteria from infected locations is a net antimicrobial effect that may occur [13]. Conversely, if bystander-induced pathogenesis is prevalent, a severe infection outcome is expected. Understanding the bystander phenomena is important, because it provides an estimate for microbial pathogenesis and prognosis. Thus, bystander effects establish the new paradigm that should be considered in assessing the response of microorganisms to therapeutic interventions, including aPDT.

Bystander parameters are cell specific items that contribute to the characterization of the sensitivity of the cells and average cell survival. They depend on the ability of targeted cells to release signals, including toxic substances or survival signals, the diffusibility of the signals, and the aptitude of cells receiving the signals to respond [17,19]. It suggests that quorum sensing (QS), bacterial cell-to-cell communication, could

be involved in mediating the bystander effects [20].

In a QS system, *A. actinomycetemcomitans* produces and detects a small molecule signal/ mediator, acyl homoserine lactone (AI-2), which potentially accumulates around the microbial cells and relays information about neighbors and allows them to synchronize their behavior. Various collaborative processes such as numerous virulence-related products including regulation of efflux pumps, metabolic activity, and cell survival are regulated in response to the AI-2 and has been shown to be important for *A. actinomycetemcomitans* pathogenesis in various model infection systems [21–25]. In *A. actinomycetemcomitans*, efflux pumps are involved in the extrusion of LtxA, as the main virulence factor, and resistance to antimicrobial agents [26,27]. The role of efflux pumps in metabolic activity and microbial cell growth was also supported in a study by Ding et al. [28] that demonstrated mutations in the efflux pump encoding genes in *A. actinomycetemcomitans* reduce the bacterial metabolism and growth capabilities. Thus, it would be very desirable to provide therapeutic strategies that can be applied to oral diseases and can suppress the microbial virulence features controlled by the QS system.

Yet, no study has investigated the effects of targeted photodynamic stress on bystander microbial cells and its role in the pathogenesis of model microorganisms in periodontitis and peri-implantitis following aPDT. Consequently, the aim of this study was to investigate the role of bystander effects in the microbial cell survival, metabolic activity, efflux capacity, and QS ability of *A. actinomycetemcomitans* following aPDT using Cur.

2. Materials and methods

2.1. Test microorganism and growth conditions

A. actinomycetemcomitans ATCC 33384 strain was cultured on sheep blood agar plates containing brain heart infusion (BHI) (Merck, Darmstadt, Germany) as the base medium supplemented with 0.5% defibrinated sheep blood, 0.6% yeast extract, 5 mg/L hemin, and 1 mg/L menadione (all three purchased from Merck, Darmstadt, Germany) at 37 °C for 48 h under microaerophilic conditions.

For experiments requiring bacterial suspension, fresh colonies grown in the supplemented BHI (sBHI) agar plate were transferred to sBHI broth and incubated at 37 °C under microaerophilic conditions in a shaker incubator at 120 rpm to achieve an optical density (OD) of 0.08–0.13, which was equal to 1.5×10^8 colony forming units (CFUs)/mL [29].

2.2. Preparation of photosensitizer stock and light source

Cur (Sigma-Aldrich Co., Ltd., Dorset, United Kingdom) stock in dimethyl sulfoxide (DMSO; 0.05 M; Sigma-Aldrich Co., Ltd., Dorset, United Kingdom) at a concentration of 80 µg/mL was used as a photosensitizer in this study. Before experiments, a sterile stock of Cur was prepared using a filtering method with a 0.22 µm filter and kept in a dark place until the exact time of experiment [30]. Light-emitting diode (LED; DY400-4, Denjoy Dental Co., Ltd., Shenzhen, China) was used as the corresponding light source to activate Cur (wavelength = 435 ± 20 nm, output intensity = 1000–1400 mW/cm²).

2.3. Experimental design

To evaluate the role of the bystander effects in the microbial cell survival, metabolic activity, efflux capacity, and QS ability of *A. actinomycetemcomitans* following aPDT using Cur, the following groups were used:

A.) WBCS^T; Whole bacterial cell suspension from *A. actinomycetemcomitans* culture treated with Cur-aPDT (T stands for "treated *A. actinomycetemcomitans* culture")

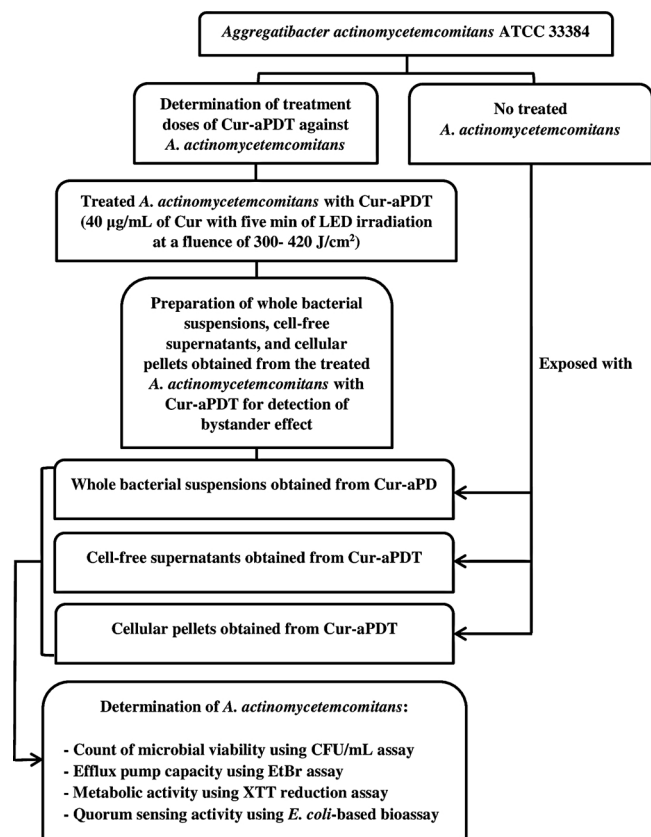


Fig. 1. Flowchart of the testing steps in the current study.

- B.) WBCS^U; Whole bacterial cell suspension from untreated *A. actinomycetemcomitans* culture (as control for group A; U stands for “untreated *A. actinomycetemcomitans* culture”).
- C.) CFSF^T; Cell-free supernatant fluid from *A. actinomycetemcomitans* culture treated with Cur-aPDT.
- D.) CFSF^U; Cell-free supernatant fluid from untreated *A. actinomycetemcomitans* culture (as control for group C).
- E.) BCP^T; Bacterial cell pellet from *A. actinomycetemcomitans* culture treated with Cur-aPDT.
- F.) BCP^U; Bacterial cell pellet from untreated *A. actinomycetemcomitans* culture (as control for group E).

2.4. Treatment doses of Cur-aPDT

The treatment dose of Cur-aPDT for *A. actinomycetemcomitans* culture was determined as described previously [31]. The treatment dose of Cur-aPDT for the test strain was 40 µg/mL of Cur + LED irradiation for 5 min at a fluence of 300–420 J/cm². The flowchart of the experiment steps is shown in Fig. 1.

2.5. Effects of bystander following Cur-aPDT on the cell survival of *A. actinomycetemcomitans*

2.5.1. Treatment of *A. actinomycetemcomitans*

First, 100 µL of the *A. actinomycetemcomitans* suspension at a concentration of 10⁶ CFU/mL was added to the wells of a flat-bottom 96-well microplate (TPP, Trasadingen, Switzerland), and then 100 µL of Cur at a concentrations of 80 µg/mL was added. After that, the microplates were placed in the dark for 5 min followed by exposure to LED radiation for 5 min as a wavelength corresponding to the Cur-aPDT procedure.

2.5.2. Preparation of CFSFs and BCPs from WBCS^T and WBCS^U

For the preparation of CFSF^T and CFSF^U, the collected contents of the wells containing WBCS^T and WBCS^U were centrifuged at 13,000 rpm at 4 °C for 20 min. CFSF^T and CFSF^U were sterilized by filtration (pore diameter of 0.22 µm). The remaining pellets were re-suspended in phosphate buffered saline (PBS) for preparation of BCP^T and BCP^U. All preparations of the Cur-aPDT-treated culture (i.e. WBCS^T, CFSF^T, and BCP^T) and the untreated culture (i.e. WBCS^U, CFSF^U, BCP^U) were stored at 4 °C until use.

2.5.3. Assessment of bystander effects induced by WBCS^T, CFSF^T, BCP^T on the cell survival of *A. actinomycetemcomitans*

To determine the bystander effect induced by WBCS^T, microbial viability assay was done using transwell assay [10]. Briefly, immediately after preparation of WBCS^T, 235 µL of treated *A. actinomycetemcomitans* was placed in the wells (diameter 4.26 mm) of a 96-well plate (Life Sciences, Beiijing, China) at a density of 10⁶ CFU/mL. To study the bystander effects, 75 µL of untreated *A. actinomycetemcomitans* culture (10⁶ CFU/mL) was transferred to a transwell culture insert dish (Life Sciences, Beijing, China). The bottom of the transwell culture insert dish has a membrane with 1 µm pores, allowing the transfer of dissolved compounds in the medium without contact between bystander and targeted bacterial cells. The plates with targeted (well) and bystander bacterial cells (insert) were then incubated at 37 °C under microaerophilic conditions and the bystander bacterial cell growth and concentration was assessed after 48 h incubation by plating 10-fold dilutions on the sBHI agar. Next, 100 µL of *A. actinomycetemcomitans* at a concentration of 10⁶ CFU/mL was poured into the microplate wells, and then 100 µL of CFSF^T obtained in Section 2.5.2 was added to this content. In the next step, microbial viability assay was performed according to a previously reported method [32]. Briefly, each bacterial growth and concentration was quantified after 48 h incubation at 37 °C by plating 10-fold dilutions on sBHI agar. Determination of the bystander effects induced by BCP^T was done as described for WBCS^T except for replacing WBCS^T with BCP^T obtained in Section 2.5.2. Then, 100 µL of WBCS^U (10⁶ CFU/mL), CFSF^U (10⁶ CFU/mL), and BCP^U were used as control groups.

2.6. Assessment of bystander effects induced by WBCS^T, CFSF^T, and BCP^T on metabolic activity of *A. actinomycetemcomitans* using XTT reduction assay

The metabolic activity of *A. actinomycetemcomitans* exposed to WBCS^T, CFSF^T, and BCP^T obtained in Section 2.5.2 was examined using the XTT (2,3-bis [2-methoxy-4-nitro-5-sulphophenyl]-2H-tetrazolium-5-carboxanilide) (Sigma Aldrich, Steinheim, Germany) reduction assay separately, as described by Coraça-Hubér et al. [33]. The XTT assay is based on the cleavage of the tetrazolium salt XTT (yellow) to form a formazan dye (orange) by metabolically active bacterial cells [34,35]. Filter-sterilized XTT (1 mg/mL in PBS) and menadione (1 mM in acetone) solutions were prepared immediately before each assay. Following each treatment under identical conditions to those described in Section 2.5.2, the content of wells was collected into 1.5 mL microtubes and centrifuged at 1500 rpm for 15 min. The resulting bacterial cell sediments were dissolved in 12 µL of XTT-menadione-PBS solution in microplate wells. Following incubation of the microplate in the dark at 37 °C for 3 h, 100 µL of the content was transferred to a new microplate and the optical intensity was determined by an automatic microplate reader (BioTek, USA) at 492 nm. WBCS^U, CFSF^U, and BCP^U were used as control groups. The percentage of metabolic activity was calculated as described previously [36,37].

2.7. Assessment of bystander effects induced by WBCS^T, CFSF^T, and BCP^T on activity of efflux pump using ethidium bromide (EtBr) assay

Efflux pump inhibition in *A. actinomycetemcomitans* following

exposure to WBCS^T, CFSF^T, and BCP^T was determined by an EtBr whole cell accumulation assay, as described previously [8]. In brief, 300 µL of mid-logarithmic phase *A. actinomycetemcomitans* (10⁶ CFU/mL) was exposed to WBCS^T, CFSF^T, or BCP^T obtained in section 2.5.2 or phenyl-arginine-β-naphthylamide (PaβN; 25 µg/mL), an efflux pump inhibitor (EPI), under identical conditions to those described in Section 2.5.3. After that, the collected content of the wells was centrifuged at 1500 rpm for 15 min and the sediment was re-suspended in PBS (300 µL). EtBr (4 µg/mL), as an efflux pump substrate, was added to 96-well plates containing 100 µL of treated *A. actinomycetemcomitans* with WBCS^T, CFSF^T, and BCP^T and PaβN. The change of the fluorescence intensity was recorded using a microplate reader in the excitation and emission wavelengths at 530 and 600 nm, respectively. The initial baseline fluorescence and the changes of EtBr fluorescence intensity were recorded within the first 30 s and 360 s of EtBr addition, respectively. In this assay, WBCS^U, CFSF^U, and BCP^U were used as control groups.

2.8. Assessment of bystander effects induced by WBCS^T, CFSF^T, and BCP^T on the QS ability of *A. actinomycetemcomitans*

Treated *A. actinomycetemcomitans* with WBCS^T, CFSF^T, and BCP^T were assayed for QS (AI-2) activity as compared with their respective controls (WBCS^U, CFSF^U, and BCP^U, respectively) using *Escherichia coli*-based bioassay systems [38,39]. *E. coli* DH5α containing pUC19 reporter plasmid that can produce β-galactosidase (LacZ) (although β-galactosidase production can be increased by incubation with an external source of AI-2) was used to quantify the QS ability of treated *A. actinomycetemcomitans*. The QS ability of the treated *A. actinomycetemcomitans* was measured by a colorimetric (β-galactosidase activities) method [40]. For this purpose, the AI-2 extraction of treated *A. actinomycetemcomitans* was performed as described previously [41]. Briefly, treated *A. actinomycetemcomitans* was grown overnight in Muller-Hinton broth (Merck, Germany) at 37 °C and then centrifuged at 10,000 rpm for 15 min. The collected supernatants were filtered through 0.22 µm membrane filters to remove cell debris. Then, the preparations were mixed with ethyl acetate and shaken for 10 min at room temperature. The upper part (organic) of the mixture was collected after 5 min in sterile tubes and dried in an oven at 40 °C. Next, 50 µL of each preparation was proceeded by liquid-liquid extraction (LLE) [42] and transferred into wells of flat-bottom 96-well microplates containing 50 µL of a 1:1 mixture of 2 M hydroxyl amine: 3.5 M NaOH. Subsequently, the same amount of 1:1 mixture of 95% ethanol: ferric chloride (10% in 4 M HCl) was added. The extracts containing probable AI-2 were concentrated in an oven at 40 °C overnight and were then used for β-galactosidase assay.

β-galactosidase activity was determined based on the Miller [43] procedure with modifications made by Stachel et al. [44] as described previously [40]. Briefly, a treated fresh culture (OD₆₀₀: 0.6–1.0) of *E. coli* DH5α harboring the pUC19 with extracts containing probable AI-2 was centrifuged and re-suspended in 500 µL of GUS buffer (1 mM EDTA, 14.3 mM 2-mercaptoethanol, 50 mM sodium phosphate pH 7.0). Then, 25 µL of 3% sodium lauryl sarcosinate in GUS buffer and 25 µL of 3% Triton X-100 in GUS buffer were added to the suspensions, the samples were incubated at 30 °C for 10 min, and then 100 µL of p-nitrophenyl-β-D-glucuronic acid (PNPG; 25 mM) was added. The reactions of the preparations were stopped by adding 280 µL of Na₂CO₃ (1 M) after developing a yellow color (10 min). Cell-free culture fluids were prepared by filtration of the suspension.

The optical density of the yellow color intensity in filtered cell-free culture fluids developed by the β-glucuronidase reaction was measured at 415 nm (OD₄₁₅PNPG). The optical density of the bacterial culture was also measured at 595 nm (OD₅₉₅).

One Miller unit (Mu) of β-glucuronidase activity was defined as follows: one Mu = 1000 × [(OD₄₁₅PNPG – (1.75 × OD₅₉₅)] / (t × v × OD₅₉₅), where t and v stand for time of reaction (in min), and

volume (mL) of the culture assayed respectively, 1.75 is the correction factor, and OD₅₉₅ is the bacterial cell density just before the assay. The assay values reported were the averages of 3 replicates.

2.9. Determination of protease, pH, and temperature stability of bystander effectors

Protease, pH, and temperature stability of bystander effectors were determined by evacuating the bystander activity of all three preparations of Cur-aPDT-treated cultures (i.e. WBCS^T, CFSF^T, and BCP^T) using the microbial viability assay against *A. actinomycetemcomitans* [44]. The heat stability of bystander effectors was evaluated by incubating WBCS^T, CFSF^T, and BCP^T in a water bath at 50 ± 1 °C for 1 h and cooling on ice separately. As control, WBCS^T, CFSF^T, and BCP^T were incubated at 37 ± 2 °C for 1 h, a treatment which did not impair the bystander effectors. Then, the heated and control WBCS^T, CFSF^T, and BCP^T were incubated (1:1 v/v) with *A. actinomycetemcomitans* (10⁶ CFU/mL) and bacterial growth and concentration were quantified after 48 h incubation at 37 °C by plating 10-fold dilutions on sBHI agar. For evaluation of the protease sensitivity of bystander effectors, proteinase K (Sigma-Aldrich Co., Ltd., Dorset, United Kingdom) was added to aliquots of WBCS^T, CFSF^T, and BCP^T at a final concentration of 1 mg/mL and the reactions were processed at 37 °C for 1 h. As control, WBCS^T, CFSF^T, and BCP^T were separately incubated at 37 ± 2 °C for 1 h without proteinase K. Microbial viability assay was done as described above.

To investigate the effect of different pH-values (pH = 5–9) on the bystander activity of WBCS^T, CFSF^T, and BCP^T, the aliquots had pH-values adjusted in a range of 5–9 using either sterile 1 M NaOH or 1 M HCl. Fresh BHI broth adjusted to the same pH-values was used as a control. Aliquots at different pH-values were incubated (1:1 v/v) with *A. actinomycetemcomitans* (10⁶ CFU/mL) for microbial viability assay as described above.

2.10. Statistical analyses

Each experiment in this study was replicated three times independently. SPSS software (version 22.0), one-way ANOVA, and Bonferroni Post Hoc tests were used for data analysis. The significance level was set at P < 0.05.

3. Results

3.1. Bystander effects change the cell survival of the *A. actinomycetemcomitans*

As shown in Fig. 2a, the cell survival of *A. actinomycetemcomitans* decreased by 82.7% (P = 0.001) and 76.2% (P = 0.01) after exposure to WBCS^T and CFSF^T, respectively compared to the corresponding control group (untreated bacteria). By contrast, there was an insignificant increase of 5.5% (P = 0.7) in the number of *A. actinomycetemcomitans* after exposure to BCP^T compared to the control group. Inter-group pair-wise comparison with Bonferroni Post Hoc test showed a statistically significant difference in the number of *A. actinomycetemcomitans* exposed to the WBCS^T and CFSF^T (P = 0.001), as well as the number of *A. actinomycetemcomitans* exposed to CFSF^T and BCP^T (P = 0.01). According to the Bonferroni Post Hoc test, there was a non-significant difference in the number of *A. actinomycetemcomitans* exposed to WBCS^T and CFSF^T (P > 0.05). Thus, cell survival of *A. actinomycetemcomitans* was affected by the bystander effects of WBCS^T and CFSF^T.

3.2. Bystander effects change cell metabolic activity in *A. actinomycetemcomitans*

We further examined the association of bystander effects with the

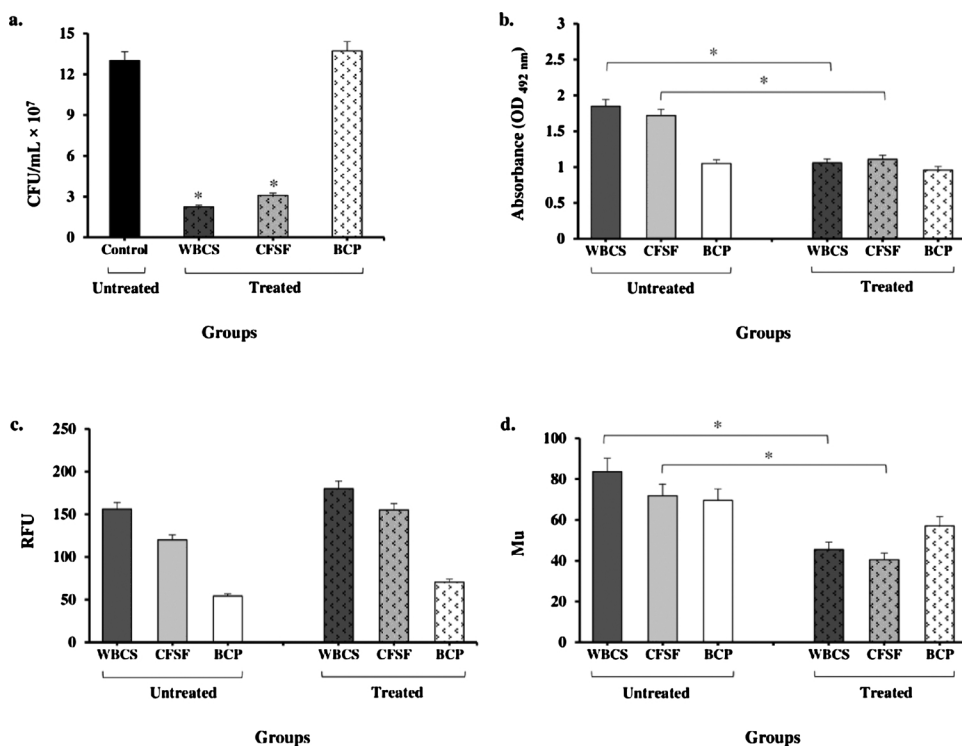


Fig. 2. Bystander effects induced by WBCS^T, CFSF^T, and BCP^T from the treated bacteria with Cur-aPDT on a) cell survival; colony forming units (CFU)/mL, b) metabolic activity; optical density (OD), c) efflux pumps capacity; relative fluorescence units (RFU), and d) levels of autoinducer-2 (AI-2) production in Miller unit (Mu) as a quorum sensing ability of *A. actinomycetemcomitans*.

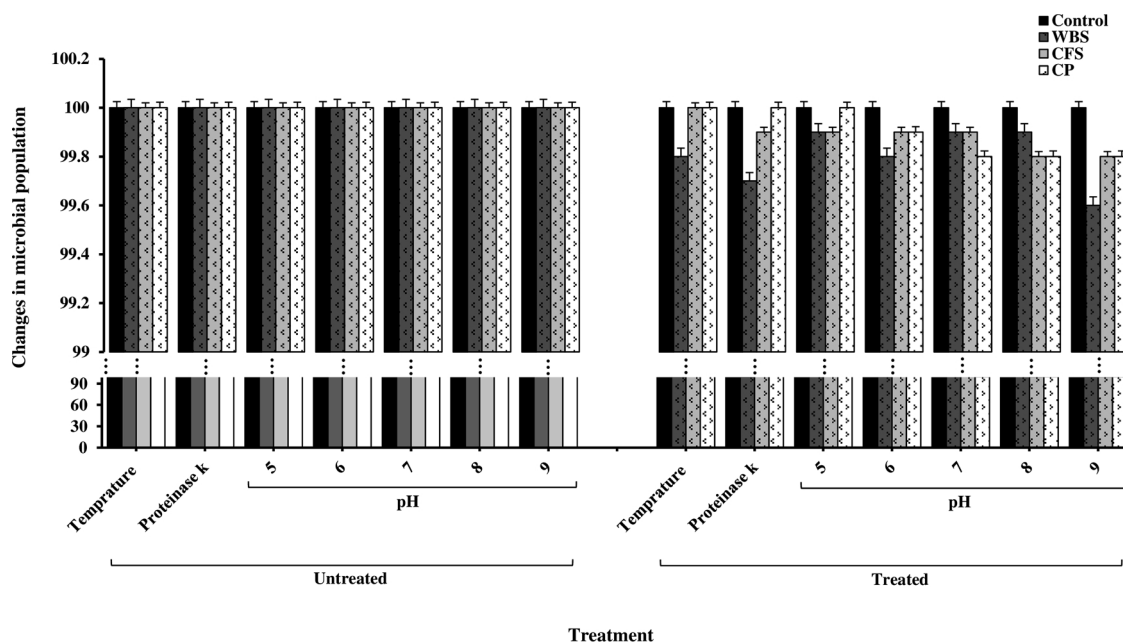


Fig. 3. Cell survival of *A. actinomycetemcomitans* after exposure with treated WBCS^T, CFSF^T, and BCP^T with different pH-values (5–9), heat (1 h at 50 ± 2 °C) and proteinase K (1 h at 37 ± 2 °C).

cell metabolic activity as a criterion for biofilm formation of *A. actinomycetemcomitans*. As shown in Fig. 2b, the metabolic activity of *A. actinomycetemcomitans* significantly reduced by 1.06 OD (42.6% reduction; P = 0.02) and 1.11 OD (35.3% reduction; P = 0.03) after exposure to WBCS^T and CFSF^T compared to the corresponding control groups (WBCS^U, and CFSF^U), respectively. It should be noted also that the metabolic activity of *A. actinomycetemcomitans* was less susceptible to BCP^T (0.96 OD; 9.4% reduction; P = 0.5) compared to the BCP^U as the control group. According to Fig. 2b, the Bonferroni Post Hoc test showed a significant difference in the metabolic activities of *A. actinomycetemcomitans* exposed to WBCS^T and CFSF^T, versus the metabolic

activity of the test bacterial strain that was treated with BCP^T (P > 0.05).

3.3. Bystander effects change the cell efflux activity in *A. actinomycetemcomitans*

Fig. 2c demonstrates the effect of treatments on cell accumulation of EtBr in *A. actinomycetemcomitans*. EtBr accumulation showed no significant difference in all three preparations of the Cur-aPDT-treated culture (i.e. WBCS^T, CFSF^T, and BCP^T) compared to their respective controls (P > 0.05; Fig. 2c). Intergroup pair-wise comparison of

WBCS^T, CFSF^T, and BCP^T showed a non-significant difference in EtBr accumulation in *A. actinomycetemcomitans*.

3.4. Bystander effects change the QS ability in *A. actinomycetemcomitans*

The QS ability (levels of AI-2 production as a QS mediator) in the treated *A. actinomycetemcomitans*, which was quantified using the reporter strain *E. coli* DH5 α harboring pUC19, is shown in Fig. 2d. There was a 45.5 Mu reduction in AI-2 produced by *A. actinomycetemcomitans* after exposure to WBCS^T. Likewise, a 40.5 Mu AI-2 reduction was observed in the *A. actinomycetemcomitans* culture treated with CFSF^T. BCP^T-treated *A. actinomycetemcomitans* produced high levels of AI-2 (57.1 Mu; $P = 0.09$) compared to the respective control group (BCP^U). *A. actinomycetemcomitans* exposed to WBCS^T, CFSF^T, and BCP^T showed a reduction of 83.2% ($P = 0.001$), 77.2% ($P = 0.01$), and 21.9% ($P = 0.09$) in AI-2 compared to the corresponding control groups (WBCS^U, CFSF^U, and BCP^U, respectively).

3.5. Protease, pH, and temperature stability of bystander effectors

As shown in Fig. 3, the cell survival of *A. actinomycetemcomitans* treated with WBCS^T, CFSF^T, and BCP^T was maintained at pH-values of 5–9. WBCS^T, CFSF^T, and BCP^T treated with heat and proteinase K for 1 h at $50 \pm 2^\circ\text{C}$ and $37 \pm 2^\circ\text{C}$, respectively showed no change in the cell survival of *A. actinomycetemcomitans*.

4. Discussions

Cell exposure to the resulting effectors of the treated cells shows biological changes called bystander effects [31]. Bystander effects can play their role by effector molecules vulnerable to genetic damages, such as chromosome mutation as well as changes in the RNA level, gene expression, and protein level, resulting in shortening the cellular life in non-target adjacent cells, known as bystander cells [45,46]. Investigation of bystander effects on cancer cells has shown that effectors, such as anti-inflammatory cytokines including IFN γ , TNF α , and IL-1, death ligands, ROS/NOS, P53, NO, microRNA, P13 K, EV, HSPs, NF- κ B, GADPH, COX2, and MARK are responsible for creating this phenomenon [45–48]. Based on the fact that no study was conducted to examine the role of bystander effects in prokaryotic cells and their bystander effectors have not been identified yet, it can be the focus of new studies.

It has been revealed that effectors could influence the bystander cells through cell-to-cell physical contact or released soluble substances from treated cells away from bystander cells [9]. Bystander effects have been extensively studied in some fields such as brain cancer [49,50], breast cancer [51], and lung cancer [52] under the title of adjacent effect caused by radiation or radiation-induced bystander effects (RIBE). The bystander response spectrum in cancer cells varies from increased proliferation, increased invasive properties, induction of resistance of tumor cells, DNA damage following radiation exposure, apoptosis induction, and shortened life and removal of tumor cells [53]. It has been reported that sub-toxic doses of nitric oxide on bystander cells in human breast cancer can increase cellular resistance to killing in PDT due to the suppression of pro-apoptotic agents and less DNA damage in the bystander cells [54].

To the best of our knowledge, no studies have investigated the role of aPDT-induced bystander effects on prokaryotic cells; therefore, this is the first report of the role of the bystander effects deriving from treated microbial cells following aPDT. The present study was based on a study conducted by Tedijanto et al. [13] that investigated the antibiotics-resistant phenotype in bystander microbial cells. They demonstrated that bystander exposure, reduced the need for antibiotic administration in *E. coli* and *Staphylococcus aureus* infection by 100% and 91%, respectively due to pneumococcal vaccination although these bacteria were not targeted by the pneumococcal conjugate vaccine [13].

Different parts of Cur-aPDT treated *A. actinomycetemcomitans* culture in the current study, particularly WBCS^T and CFSF^T, demonstrated significant changes in microbial cell survival, metabolic activity, and QS processes of *A. Actinomycetemcomitans* in the aPDT-induced bystander effects. This may suggest that metabolites with bystander properties that are produced by Cur-aPDT treated *A. actinomycetemcomitans* are more likely to be secreted to the culture supernatant. By contrast, the crude cell extract of Cur-aPDT treated *A. actinomycetemcomitans* had a very little bystander effects on *A. actinomycetemcomitans*. This is probably owing to the loss of bystander effectors of microbial crude cell extract during the preparation process, or they may have never been present in the microbial cell structure.

Considering the differences in cell types and treatments, the statistically insignificant increase of bystander cell survival of *A. actinomycetemcomitans* following exposure to BCP^T was not in line with the results of a study by Dabrowska et al. [55]. In this research, Dabrowska et al. [55] found that adding cells receiving PDT could significantly reduce the mitotic activity of the bystander cells of ovarian cancer. Altogether, it could be concluded that BCP^T is incapable of inducing bystander effects on the cell survival of *A. actinomycetemcomitans*.

Previous investigations have shown that the metabolic activity of microbial cells tend to adhere to the surface due to accumulation of nutrients in the extracellular polymeric substances matrix on the surface, which contributes to their bacterial growth rate, biofilm formation ability, and pathogenic activity [56,57]. Here, we presented evidence suggesting that the development of bystander effects due to Cur-aPDT may also reduce the metabolic activity in *A. actinomycetemcomitans*, which in turn might reduce the ability of biofilm formation and impair bacterial persistence in the infection site. Since reduced metabolic activity has been shown to decrease the division rate, attachment, and formation of biofilm and cause structural changes in the pathogenicity of microbial cells, it could be proposed that during Cur-aPDT treatment, bystander effectors can lead to decreased fitness and lower *A. actinomycetemcomitans* virulence over time.

Efflux pumps are ubiquitous among bacteria and their role in protein secretion and discharge antimicrobial compounds has been well established [26]. In the current study, the bystander effects induced by the WBCS^T, CFSF^T, and BCP^T showed no effect on the efflux pump activity and accumulation of an efflux pump substrate, EtBr, in the test bacterial strain. A low level of LtxA secretion and alteration of the drug resistance profile is typically described for mutation in genes coding efflux pumps [26]. This indicates that the bystander effects induced by Cur-aPDT does not modulate any of the factors affecting efflux pump dependent bacterial pathogenesis, including LtxA and antibiotic susceptibility.

According to the results of this study, *A. actinomycetemcomitans* treated with WBCS^T, CFSF^T, and BCP^T showed reduced AI-2 production by *E. coli*-based bioassay method in comparison with the bacteria grown without treatments. WBCS^T and BCP^T significantly reduced the level of AI-2 ($P < 0.001$). It is interesting to note that *A. actinomycetemcomitans* populations were less affected by BCP^T compared to other treatments, which can be due to the fact that BCP^T contains low concentrations of bystander effectors. The use of QS inhibitors of diverse origins has been shown to act as potential anti-pathogens [58]. Therefore, bystander effectors resulting from aPDT should be considered for further studies in this regard. To the best of our knowledge, no study has characterized the effects of bystander phenomenon resulting from aPDT as a new therapeutic modality on anti-microbial photodynamic treatment.

The preliminary study of bystander effectors originating from *A. actinomycetemcomitans* treated with Cur-aPDT produced thermo-stable, acid and alkaline resistant, non-proteinaceous molecules that showed different origin-dependent behaviors against untreated bacteria. In this study, bioactive components of WBCS^T, CFSF^T, and BCP^T were not inactivated after treatment with heat and proteinase K at $50 \pm 1^\circ\text{C}$ and $37 \pm 2^\circ\text{C}$ for 1 h, respectively and pH-values ranging from 5 to 9 and their anti-microbial activity were preserved.

5. Conclusions

The results of the current study revealed that Cur-aPDT could significantly reduce the microbial population, cell metabolic activity and efflux pump capacity through bystander effects on untreated bacterial cells. As a result, bystander effects produced by Cur-aPDT along with the direct effect of aPDT can enhance the efficiency of aPDT as a therapeutic method for the treatment of local infections. Based on these findings, the concentration of photosensitizer applied to site of infection and the intensity of irradiation should be considered as crucial factors in the aPDT procedure in local infection situations.

Conflict of interest

The authors declare that there is no conflict of interests regarding the publication of this paper.

Acknowledgement

This research has been supported by Tehran University of Medical Sciences & Health Services grant No. 96-04-30-36992.

References

- M.S. Tonetti, S. Jepsen, L. Jin, J. Otomo-Corgel, Impact of the global burden of periodontal diseases on health, nutrition and wellbeing of mankind, a call for global action, *J. Clin. Periodontol.* 44 (2017) 456–462.
- R. Smeets, A. Henningsen, O. Jung, M. Heiland, C. Hammächer, J.M. Stein, Definition, etiology, prevention and treatment of peri-implantitis—a review, *Head Face Med.* 10 (2014) 34.
- N.T. Hashim, G.J. Linden, L. Winning, M.E. Ibrahim, B.G. Gismalla, F.T. Lundy, et al., Putative periodontal pathogens in the subgingival plaque of Sudanese subjects with aggressive periodontitis, *Arch. Oral Biol.* 81 (2017) 97–102.
- B. Benso, Virulence factors associated with *Aggregatibacter actinomycetemcomitans* and their role in promoting periodontal diseases, *Virulence* 8 (2017) 111–114.
- F. Ahrari, K. Ghazvini, F. Mazhari, R. Fekrazad, N. Eslami, N. Emrani, Evaluation of the effect of antimicrobial photodynamic therapy on *Streptococcus mutans*—an in vitro study, *J. Mash. Dent. School* 40 (2016) 105–112.
- L. Chambrone, H.L. Wang, G.E. Romanos, Antimicrobial photodynamic therapy for the treatment of periodontitis and peri-implantitis: an American Academy of Periodontology best evidence review, *J. Periodontol.* 89 (2018) 783–803.
- S. Rajesh, E. Koshi, K. Philip, A. Mohan, Antimicrobial photodynamic therapy: an overview, *J. Indian Soc. Periodontol.* 15 (2011) 323.
- M. Pourhajbagher, E. Boluki, N. Chiniforush, B. Pourakbari, Z. Farshadzadeh, R. Ghorbanzadeh, et al., Modulation of virulence in *Acinetobacter baumannii* cells surviving photodynamic treatment with toluidine blue, *Photodiagn. Photodyn. Ther.* 15 (2016) 202–212.
- D.P. Leite, F.R. Paolillo, T.N. Parmesano, C.R. Fontana, V.S. Bagnato, Effects of photodynamic therapy with blue light and curcumin as mouth rinse for oral disinfection: a randomized controlled trial, *Photomed. Laser Surg.* 32 (2014) 627–632.
- A. Chakraborty, K.D. Held, K.M. Prise, H.L. Liber, R.W. Redmond, Bystander effects induced by diffusing mediators after photodynamic stress, *Radiat. Res.* 172 (2009) 74–81.
- C. Mothersill, C. Seymour, Are epigenetic mechanisms involved in radiation-induced bystander effects? *Front. Genet.* 3 (2012) 74.
- B.J. Blyth, P.J. Sykes, Radiation-induced bystander effects: what are they, and how relevant are they to human radiation exposures? *Radiat. Res.* 176 (2011) 139–157.
- C. Tedijanto, S. Olesen, Y. Grad, M. Lipsitch, Estimating the Proportion of Bystander Selection for Antibiotic Resistance Among Potentially Pathogenic Bacterial Flora, *USbioRxiv*, 2018 [Head of press].
- P.J. Warburton, R.M. Palmer, M.A. Munson, W.G. Wade, Demonstration of in vivo transfer of doxycycline resistance mediated by a novel transposon, *J. Antimicrob. Chemother.* 60 (2007) 973–980.
- A.P. Roberts, J. Kreth, The impact of horizontal gene transfers on the adaptive ability of the human oral microbiome, *Front. Cell. Infect. Microbiol.* 4 (2014) 124.
- A.P. Roberts, P. Mullany, Oral biofilms: a reservoir of transferable, bacterial, antimicrobial resistance, *Expert Rev. Anti Infect. Ther.* 8 (2010) 1441–1450.
- V. Peng, N. Suchowerska, L. Rogers, E. Claridge Mackonis, S. Oakes, D.R. McKenzie, Grid therapy using high definition multileaf collimators: realizing benefits of the bystander effect, *Acta Oncol.* 56 (2017) 1048–1059.
- M. Pourhajbagher, A. Bahador, Gene expression profiling of fimA gene encoding fimbriae among clinical isolates of *Porphyromonas gingivalis* in response to photo-activated disinfection therapy, *Photodiagn. Photodyn. Ther.* 20 (2017) 1–5.
- V. Peng, N. Suchowerska, A.D.S. Esteves, L. Rogers, E. Claridge Mackonis, J. Toohy, et al., Models for the bystander effect in gradient radiation fields: range and signalling type, *J. Theor. Biol.* 455 (2018) 16–25.
- T. Defoirdt, Quorum-sensing systems as targets for antivirulence therapy, *Trends Microbiol.* 26 (2018) 313–328.
- E.A. Novak, H. Shao, C.A. Daep, D.R. Demuth, Autoinducer-2 and QseC control biofilm formation and in vivo virulence of *Aggregatibacter actinomycetemcomitans*, *Infect. Immun.* 78 (2010) 2919–2926.
- B. Subhadra, D.H. Kim, K. Woo, S. Surendran, C.H. Choi, Control of biofilm formation in healthcare: recent advances exploiting quorum-sensing interference strategies and multidrug efflux pump inhibitors, *Materials (Basel)* 11 (2018) 1676.
- H. Shao, R.J. Lamont, D.R. Demuth, Autoinducer 2 is required for biofilm growth of *Aggregatibacter (Actinobacillus) actinomycetemcomitans*, *Infect. Immun.* 75 (2007) 4211–4218.
- K. Bao, N. Bostanci, N. Selevsek, T. Thurnheer, G.N. Belibasakis, Quantitative proteomics reveal distinct protein regulations caused by *Aggregatibacter actinomycetemcomitans* within subgingival biofilms, *PLoS One* 10 (2015) 0119222.
- D. James, H. Shao, R.J. Lamont, D.R. Demuth, The *Actinobacillus actinomycetemcomitans* ribose binding protein RbsB interacts with cognate and heterologous autoinducer 2 signals, *Infect. Immun.* 74 (2006) 4021–4029.
- J.A. Crosby, S.C. Kachlany, T.deA, a TolC-like protein required for toxin and drug export in *Aggregatibacter (Actinobacillus) actinomycetemcomitans*, *Gene* 388 (2007) 83–92.
- I. Alav, J.M. Sutton, K.M. Rahman, Role of bacterial efflux pumps in biofilm formation, *J. Antimicrob. Chemother.* 73 (2018) 2003–2020.
- Q. Ding, K.S. Tan, Himar1 transposon for efficient random mutagenesis in *Aggregatibacter actinomycetemcomitans*, *Front. Microbiol.* 8 (2017) 1842.
- M. Pourhajbagher, A. Monzavi, N. Chiniforush, M.M. Monzavi, S. Sobhani, S. Shahabi, et al., Real-time quantitative reverse transcription-PCR analysis of expression stability of *Aggregatibacter actinomycetemcomitans* fimbria-associated gene in response to photodynamic therapy, *Photodiagn. Photodyn. Ther.* 18 (2017) 78–82.
- M. Pourhajbagher, N. Chiniforush, S. Parker, S. Shahabi, R. Ghorbanzadeh, M.J. Kharazifard, et al., Evaluation of antimicrobial photodynamic therapy with indocyanine green and curcumin on human gingival fibroblast cells: an in vitro phototoxicity investigation, *Photodiagn. Photodyn. Ther.* 15 (2016) 13–18.
- M. Pourhajbagher, N. Chiniforush, A. Monzavi, H.R. Barikani, M.M. Monzavi, Sh. Sobhani, et al., Inhibitory effects of antimicrobial photodynamic therapy with curcumin on biofilm-associated gene expression profile of *Aggregatibacter actinomycetemcomitans*, *J. Dent. (Tehran)* 15 (2018) 169–177.
- P.J. Petersen, P. Labthavikul, C.H. Jones, P.A. Bradford, In vitro antibacterial activities of tigecycline in combination with other antimicrobial agents determined by checkerboard and time-kill kinetic analysis, *J. Antimicrob. Chemother.* 57 (2006) 573–576.
- D.C. Coraça-Hubér, M. Fille, J. Hausdorfer, K. Pfaller, M. Noggler, Evaluation of MBEC™-HTP biofilm model for studies of implant associated infections, *J. Orthop. Res.* 30 (2012) 1176–1180.
- G. Di Bonaventura, A. Pompilio, C. Picciani, M. Iezzi, D. D'Antonio, R. Piccolomini, Biofilm formation by the emerging fungal pathogen *Trichosporon asahii*: development, architecture, and antifungal resistance, *Antimicrob. Agents Chemother.* 50 (2006) 3269–3276.
- S.H. Subramanya, N.K. Sharan, B.P. Baral, D. Hamal, N. Nayak, P.Y. Prakash, et al., Diversity, in-vitro virulence traits and antifungal susceptibility pattern of gastrointestinal yeast flora of healthy poultry, *Gallus gallus domesticus*, *BMC Microbiol.* 17 (2017) 113.
- M. Pourhajbagher, E. Boluki, N. Chiniforush, B. Pourakbari, Z. Farshadzadeh, R. Ghorbanzadeh, et al., Modulation of virulence in *Acinetobacter baumannii* cells surviving photodynamic treatment with toluidine blue, *Photodiagn. Photodyn. Ther.* 15 (2016) 202–212.
- L.C. Oliveira, A.M.M. Silveira, A.S. Monteiro, V.L. Dos Santos, J.R. Nicoli, V.A.C. Azevedo, et al., In silico prediction, in vitro antibacterial spectrum, and physicochemical properties of a putative bacteriocin produced by *Lactobacillus rhamnosus* strain L156.4, *Front. Microbiol.* 8 (2017) 876.
- S. Chusri, I. Villanueva, S.P. Voravuthikunchai, J. Davies, Enhancing antibiotic activity: a strategy to control *Acinetobacter* infections, *J. Antimicrob. Chemother.* 64 (2009) 1203–1211.
- A.C. Joelson, J. Zhu, LacZ-based detection of acyl-homoserine lactone quorum-sensing signals, *Curr. Protoc. Microbiol.* (2006) Chapter 1: Unit 1, pp. 1–9.
- D.P. da Silva, H.K. Patel, J.F. González, G. Devescovi, X. Meng, S. Covacevzsch, et al., Studies on synthetic LuxR solo hybrids, *Front. Cell. Infect. Microbiol.* 5 (2015) 52.
- R. Taghadosi, M.R. Shakibaie, S. Masoumi, Biochemical detection of N-Acyl homoserine lactone from biofilm-forming uropathogenic *Escherichia coli* isolated from urinary tract infection samples, *Rep. Biochem. Mol. Biol.* 3 (2015) 56–61.
- Y.H. Yang, T.H. Lee, J. Kim, E.J. Kim, H.S. Joo, C.S. Lee, et al., High-throughput detection method of quorum-sensing molecules by colorimetry and its applications, *Anal. Biochem.* 356 (2006) 297–299.
- J.H. Miller, Experiments in Molecular Genetics, Cold Spring Harbor Laboratory Press, New York, NY, USA, 1972.
- S.E. Stachel, G. An, C. Flores, E.W. Nester, A Tn3 lacZ transposon for the random generation of beta-galactosidase gene fusions: application to the analysis of gene expression in *Agrobacterium*, *EMBO J.* 4 (1985) 891–898.
- V.A. Yakovlev, Role of nitric oxide in the radiation-induced bystander effect, *Redox Biol.* 6 (2015) 396–400.
- B.J. Blyth, P.J. Sykes, Radiation-induced bystander effects: what are they, and how relevant are they to human radiation exposures? *Radiat. Res.* 176 (2011) 139–157.
- C. Shao, J. Zhang, K.M. Prise, Differential modulation of a radiation-induced bystander effect in glioblastoma cells by pifithrin- α and wortmannin, *Nucl. Instrum. Methods Phys. Res. B* 268 (2010) 627–631.
- K.M. Prise, J.M. O'Sullivan, Radiation-induced bystander signalling in cancer therapy, *Nat. Rev. Cancer* 9 (2009) 351–360.

- [49] D. Zhang, T. Zhou, F. He, Y. Rong, S.H. Lee, S. Wu, et al., Reactive oxygen species formation and bystander effects in gradient irradiation on human breast cancer cells, *Oncotarget* 7 (2016) 41622–41636.
- [50] W. Rong, Z. Tingyang, L. Wei, Z. Li, Molecular mechanism of bystander effects and related abscopal/cohort effects in cancer therapy, *Oncotarget* 9 (2018) 18637–18647.
- [51] S. Burdak-Rothkamm, S.C. Short, M. Folkard, K. Rothkamm, K.M. Prise, ATR-dependent radiation-induced γ H2AX foci in bystander primary human astrocytes and glioma cells, *Oncogene* 26 (2007) 993–1002.
- [52] C. Fernandez-Palomo, C. Seymour, C. Mothersill, Inter-relationship between low-dose hyper-radiosensitivity and radiation-induced bystander effects in the human T98G glioma and the epithelial HaCaT cell line, *Radiat. Res.* 185 (2016) 124–133.
- [53] F. Bewicke-Copley, L.A. Mulcahy, L.A. Jacobs, P. Samuel, N. Akbar, R.C. Pink, et al., Extracellular vesicles released following heat stress induce bystander effect in unstressed populations, *J. Extracell. Vesicles* 6 (2017) 1340746.
- [54] R. Bhowmick, A.W. Girotti, Signaling events in apoptotic photokilling of 5-amino-levulinic acid-treated tumor cells: inhibitory effects of nitric oxide, *Free Radic. Biol. Med.* 47 (2009) 731–740.
- [55] A. Dabrowska, M. Goś, P. Janik, Bystander effect induced by photodynamically or heat-injured ovarian carcinoma cells (OVP10) in vitro, *Med. Sci. Monit.* 11 (2005) 316–324.
- [56] A. Mohaghegh Motlagh, S. Pant, C. Gruden, The impact of cell metabolic activity on biofilm formation and flux decline during cross-flow filtration of ultrafiltration membranes, *Desalination* 316 (2013) 85–90.
- [57] M.C. van Loosdrecht, J. Lyklema, W. Norde, A.J. Zehnder, Influence of interfaces on microbial activity, *Microbiol. Rev.* 54 (1990) 75–87.
- [58] V.C. Kalia, S.K.S. Patel, Y.C. Kang, J.K. Lee, Quorum sensing inhibitors as anti-pathogens: biotechnological applications, *Biotechnol. Adv.* 22 (2018), <https://doi.org/10.1016/j.biotechadv.2018.11.006>.